where Q_a and Q_t are the molecular vibrational partition functions in the $^6A_1$ and $^2T_2$ states, respectively, and ΔV is the change in molar volume. The latter is an insignificant correction in the context of constant pressure measurements and will be ignored for the time being.

A convenient way of handling the now rather elaborate equation for the magnetic moment, namely equation (1) as modified by (2), is to define an equilibrium constant K_1, being the ratio of the populations in the $^6A_1$ state and the lower (doubly degenerate) component of the $^2T_2$ state. Then (neglecting ΔV)

$$\ln \tfrac{1}{3}K_1 = \ln (Q_a/Q_t) - (E+\zeta)\,(E+\zeta)/kT. \tag{3}$$

Since Q_a/Q_t is in general dependent on T, a plot of $\log K_1$ against T^{-1} should not, in general, be a straight line. We shall treat this general case shortly. First, however, it is convenient to explore a way in which the magnetic data might be fitted empirically, namely by setting

$$Q_a/Q_t = c, \quad \text{a constant.} \tag{4}$$

To do this we first assume values for g and ζ; t hese establish the relative populations of the upper and lower components of $^2T_2$. The observed values of μ^2 are then used to calculate apparent values of K_1. We consider that g should lie between 1·8 and 2·2, and ζ between 300 and 440 cm^{-1}. Using values within these limits we find it possible to obtain straight-line relations between $\log K_1$ and T^{-1} for all of the complexes studied. Three of them are shown in figure 10. These straight lines determine the constants c and $E+\zeta$, and these, when used in equations (1), (2) and (4), yield the calculated curves of figures 6 and 7. We conclude that this procedure offers a convenient semi-empirical representation of the magnetic data, within the temperature range 80 to 400 °K. The values of E required are in the expected range and fall in the order which figure 6 would lead one to expect, e.g. from figure 10, $E = 780\ \text{cm}^{-1}$ (isobutyl), $350\ \text{cm}^{-1}$ (methyl), and $-40\ \text{cm}^{-1}$ (*n*-butyl). However, not much significance is attached to these values since there is a fair latitude in the choice of g and ζ, as far as obtaining straight lines is concerned, and the choice somewhat affects E and c.

A more significant approach theoretically requires that we return to equation (3). In order to simplify the model to the limit, assume that contributions to Q_a/Q_t come only from the six Fe–S stretching vibrations and the nine S–Fe–S bending modes. Assume further that the vibrations in each class have a common frequency in each state, ν_{as} and ν_{ts} being the stretching frequencies in the $^6A_1$ and $^2T_2$ states, and ν_{ab}, ν_{tb} the corresponding bending frequencies. Then

$$\frac{Q_a}{Q_t} = \left\{\frac{1-\mathrm{e}^{-\nu_{ts}/kT}}{1-\mathrm{e}^{-\nu_{as}/kT}}\right\}^6 \left\{\frac{1-\mathrm{e}^{-\nu_{tb}/kT}}{1-\mathrm{e}^{-\nu_{ab}/kT}}\right\}^9. \tag{5}$$

We have located the metal-sulphur stretching frequency by examining first the infra-red spectra of Co (III) dimethyldithiocarbamate and its selenium analogue. In the former compound there is an absorption band at $360\ \text{cm}^{-1}$, in the latter it is missing. We take this to be the metal-sulphur stretching frequency and note that it appears in almost the same position in the vibrational spectrum of the platinum

complex as assigned by Nakamoto, Fujita, Condrate & Morimoto (1963). In our series of iron complexes (and in them only) this band is doubled, the peaks appearing in the range 300 to 400 cm^{-1} (e.g. 330 and 360 cm^{-1} for the Me_2 compound). We tentatively assign these bands to the two different states of the Fe atom and will use their frequencies for ν_{as} and ν_{ls} respectively. The bending frequencies ν_{ab} and ν_{lb} must be much lower—inaccessibly so with our instrumentation. The values $\nu_{ab} = 160$ and $\nu_{lb} = 180\ cm^{-1}$ are postulated for an illustrative calculation.

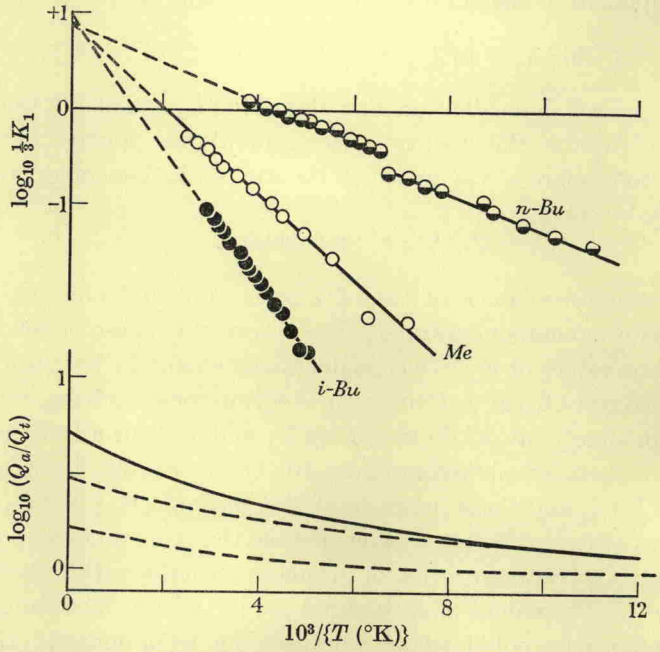

FIGURE 10. Upper curves: temperature dependence of the apparent equilibrium constant K_1, calculated using $\zeta = 370\ cm^{-1}$ and $g = 2{\cdot}00$ (for *Me* and *n-Bu*) and $g = 1{\cdot}95$ (for *i-Bu*). Lower curves: illustrative vibrational correction curves. Broken curves: stretching modes (lower) and bending modes (upper). Full curve: their sum.

In the lower part of figure 10 we plot $\log (Q_a/Q_t)$ as calculated from equation (5), using these numbers. Equation (3) then requires that it should be possible to find a vibrational correction curve (such as the curves in the lower part of the figure), which, when subtracted from a plot of $\log \frac{1}{3}K_1$ (one of the upper set of lines), yields a straight line whose intercept at $T^{-1} = 0$ is zero. The order of magnitude of the vibrational corrections is clearly sufficient to yield the correct intercept. Any slight curvature in the resulting difference plot could be accommodated by varying the choice of g or ζ from which K_1 was initially calculated, or by introducing a proper spread of vibrational frequencies rather than just two. Exact fitting of the experimental results is clearly feasible. It is equally plain, however, that no unique determination of the molecular parameters is to be expected from this approach, and this appears to be as far as the argument can be taken without the introduction of new kinds of experimental information yielding direct measures of the populations in the various levels.